Macromolecules
ARTICLE

Macromolecules **2010**, *43*, 9417–9425 **9417**
DOI: 10.1021/ma101463m

CO_2 Gas Transport Properties of Nanocomposites Based on Polyhedral Oligomeric Phenethyl-Silsesquioxanes and Poly(bisphenol A carbonate)

Ning Hao,† Martin Böhning, and Andreas Schönhals*

BAM Federal Institute for Materials Research and Testing (Department VI.5), Unter den Eichen 87, D-12200 Berlin, Germany. †Permanent address: IPG NB Design, Lenovo China; No.6 Shangdi Xilu, Haidian District, Beijing, P. R. China

Received July 8, 2010; Revised Manuscript Received October 6, 2010

ABSTRACT: Polymer-based nanocomposites were prepared by solution blending of polyhedral oligomeric silsesquioxane with phenethyl substituents (PhenethylPOSS) into poly(bisphenol A carbonate) (PBAC). First investigations focused on structure, morphology and dynamics, addressed mainly by dielectric relaxation spectroscopy are substantially extended in this study by the investigation of the CO_2 gas transport behavior of these materials, i.e., permeation experiments using the time-lag technique as well as gravimetric gas sorption measurements. The nanocomposite materials were prepared with nanofiller contents ranging from 0 to about 40 wt % by solution blending and films of about 50−100 μm thickness were cast from this solution and used for the investigation of gas transport properties after drying and annealing. From the time-lag measurements the permeability and an effective diffusion coefficient for CO_2 is obtained in dependence of POSS concentration and temperature. As main results, both, the permeability and the diffusivity, increase whereas the solubility decreases with increasing POSS concentration. These findings are discussed in the framework of a microphase separated morphology of the nanocomposite systems for POSS concentrations greater than a value c_{POSS}^{crit} of ca. 7 wt % consisting of a polycarbonate-rich matrix and POSS-rich domains which are surrounded by an interfacial layer. The experimental solubility data suggest that the POSS-rich domains are more or less impermeable for CO_2. On the basis of this assumption a quantitative model is provided to correct the solubility data for the phase separated morphology. Moreover the importance of the interfacial layer between the POSS particles or its domains for the properties of nanocomposites especially for the gas transport behavior is addressed by analyzing the sorption isotherms. Also, for the first time results from gas transport measurements and dielectric spectroscopy were quantitatively related to each other by taking the activation energies of CO_2 diffusion and of the dielectric β-relaxation into consideration. The obtained clear correlation indicates that the CO_2 gas transport is due to localized molecular fluctuations. As a further result, the diffusion coefficient obtained from time-lag and gas sorption measurements is in good agreement with respect to both their absolute values and in their concentration dependence.

1. Introduction

The synthesis and application of nanocomposites based on polymers and inorganic nanoparticles receive more and more attention from both points of view: fundamental and applied research. The latter is mainly related to the fact that due to the small size of the filler particles and its dispersion on the nanometre scale polymer-based nanocomposites can show remarkable property improvements such as increased tensile properties, decreased gas permeability, decreased solvent uptake, increased thermal stability and flame retardance etc. when compared to conventionally scaled composites. From the point of fundamental research there is a growing interest to develop new kinds of hybrid materials, to study their structure/property relationships with emphasis on influences of internal interfaces and also to investigate polymer dynamics under the conditions of severe confinement.

There are numbers of review articles available which deal with the synthesis, the characterization, and the properties of polymer nanocomposites.[1−5] In most cases these studies concentrate on the use of layered silicates (e.g., clays) as nanofillers in polymer matrices where the organically modified particles are partly or fully exfoliated and dispersed (see for instance ref 6). Among other nanoparticles (silicas, nanosized metals, nanosized carbon compounds etc.) polyhedral oligomeric silsesquioxanes (POSS[7]) is in particular interesting as nanofiller for polymer-based nanocomposites. (see, for instance, refs 8−20). POSS consists of a silica cage in the core with organic substituents R attached at the edges of the cage. Its general formula is $(SiO_{1.5})_nR_n$,[9] where n is the number of silicon atoms in the inner cage (n = 8, 10, 12, ...). Besides the fact that POSS chemically is a rather complex molecule, from a more general point of view it can be regarded as the smallest possible silica particle. Because of the attached organic substituents this silica particle is surrounded by a well-defined organic surface.[9,21] If POSS is blended into polymers, the compatibility between a "POSS nanoparticle" and different matrices can be tuned by the variation of R.[22] A quite important aspect of the blending method is to maintain a stable dispersion of the POSS molecules—first in the polymer solution and then in the resulting solid polymer matrix—on a molecular level even for higher concentrations of POSS. For instance it was reported for IsobutylPOSS/PMMA,[23] acrylic-POSS/PMMA,[24] and OctamethylPOSS/HDPE[9] that POSS can be dispersed in the matrix on a molecular level only up to a critical concentration c_{POSS}^{crit}. For higher concentrations than c_{POSS}^{crit} a phase-separated morphologies are observed. The absolute value of c_{POSS}^{crit} depends on the interaction between the POSS substituents R and the polymer

*Corresponding author. Telephone: +49 30/8104-3384. Fax: +49 30/8104-1637. E-mail: Andreas.Schoenhals@bam.de.

© 2010 American Chemical Society

Published on Web 10/25/2010

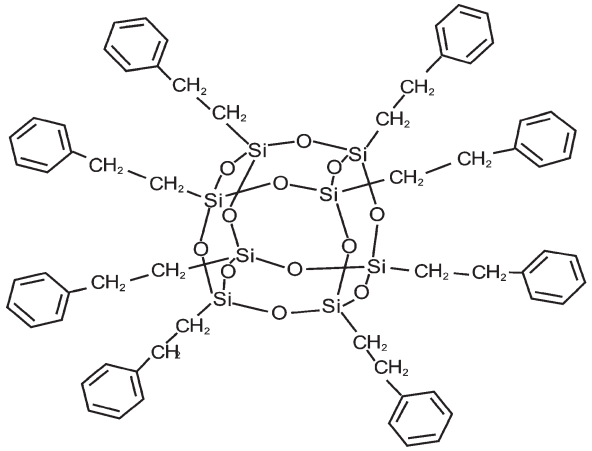

Figure 1. Chemical structure of octa-PhenethylPOSS.

segments. This was demonstrated for instance by studies considering blends of IsooctylPOSS in isotactic polypropylene[25] or PhenethylPOSS in polystyrene.[19] Recently, also molecular dynamic simulations have been used to investigate the structure property relationships of POSS-based polymeric nanocomposites.[26,27]

We reported earlier about blending PhenethylPOSS into poly(bisphenol A carbonate) (PBAC) and the resulting nanocomposites were investigated mainly by dielectric spectroscopy in detail.[20] It was shown that PhenethylPOSS can be dissolved on a molecular level into PBAC up to a critical concentration of $c_{POSS}^{crit} \approx 7-10$ wt %. For these low concentrations of the filler the main effect of POSS is a plasticization of the polymeric matrix. For higher concentrations of PhenethylPOSS a phase separation into a PBAC-rich matrix with few percents of molecularly solved POSS and POSS-rich domains is observed (see also ref 28).

Besides their relevance for practical applications such as barrier materials, coatings or membrane technology, gas transport measurements have been proven to be also a powerful tool for the characterization of polymer based nanocomposites.[29,30] It was shown that the gas transport through a polymeric matrix can be dramatically influenced by the presence of nanoparticles. The relevant aspects influencing the gas transport behavior of polymer/clay nanocomposites are comprehensively summarized in a recent review.[31] For certain nanocomposites, the unusual simultaneous increase of both permeability and permselectivity (compared to the unmodified polymer) was achieved.[30] In this study, the gas transport properties of CO_2 in PhenethylPOSS/PBAC nanocomposites are investigated by permeation and sorption measurements. Moreover for the first time dielectric and gas transport measurements for such materials are comparatively discussed and correlated to each other.

2. Experimental Section

2.1. Materials and Sample Preparation. PBAC was purchased from Sigma-Aldrich and used as matrix polymer (M_n = 22 000 g/mol, PDI = 1.23). The glass transition temperature T_g is 422 K measured by DSC (second heating run, heating rate 10 K/min).[20]

PhenethylPOSS was obtained from Hybrid Plastics, Inc. Its molecular structure is sketched in Figure 1. MALDI−TOF mass spectroscopy showed that the product is a mixture of octa-PhenethylPOSS (n = 8, T8-cage), deca-PhenethylPOSS (n = 10, T10-cage), dodeca-PhenethylPOSS (n = 12, T12-cage), and probably smaller amounts of POSS of higher cage sizes.[20] It is not possible to obtain any quantitative information about the fractions of the different cages from the intensities of the peaks of the MALDI−TOF mass spectra. But it is known that for conventional synthesis conditions the major part of the product consists of T8 cages.[32,33] PhenethylPOSS is a viscous liquid at room temperature. Because of the mixture of different cage sizes it does not crystallize but undergoes a glass transition at 243.7 K.[20] Both materials were used without any further purification.

Table 1. Composition and Sample Codes of the Investigated Nanocomposites[a]

sample code	c_{POSS} [wt %]	T_g^{DSC} [K]	ρ [g/cm^3]
PhenethylPOSS	100	243.7	1.215
PC000	0	422.0	1.196
PC002	2.4	412.3	1.178
PC005	4.8	411.0	1.180
PC010	9.1	406.5	1.180
PC013	13.0	406.2	1.182
PC017	16.7	403.0	1.206
PC023	23.1	402.4	1.209
PC029	28.6	402.4	1.211
PC033	33.3	397.7	1.212
PC041	41.2	399.4	1.209

[a] In addition its glass transition temperatures estimated by DSC and its densities are given according to ref 20.

The preparation of the nanocomposites was described in detail elsewhere.[20] In brief, during a first step PBAC was dissolved in dichloromethane (DCM) with a concentration of 20 wt %. In a second step PhenethylPOSS was dissolved/dispersed with the selected concentrations in that PBAC/DCM solution. The mixture was ultrasonificated (Bandelin Sonopuls, HD200/UW200 homogenizer equipped with KE76 titanium tapered tip) for 5 min and cast on a glass substrate by a custom-made casting knife. To control the initial evaporation of the solvent from the prepared film the glass plate was placed in a closed chamber with an atmosphere of solvent vapor. After this first evaporation step of the solvent, the films were depleted from the substrate by immersion in water. To remove the residual solvent the samples were annealed in a further step in vacuum (10^{-3} mbar) at 363 K for 24 h. This annealing temperature is below the glass transition temperature of pure polycarbonate (422 K). Gas permeation measurements require pinhole free samples with relative large plane surfaces. These requirements cannot be met by annealing the films above their glass transition temperature. Thermogravimetric analysis (TGA) was applied to check for the complete removal of the solvent. Also the glass transition temperature measured for a solvent-cast pure polycarbonate film agrees well with literature data for bulk PBAC (see Table 1).

Film thicknesses were adjusted to 50 to 100 μm. While the samples with low concentrations of PhenethylPOSS are transparent, those of higher concentrations become increasingly turbid with increasing concentration of PhenethylPOSS. This is attributed to a phase-separated morphology as discussed in reference.[20] Details of the samples under investigation including their densities reported in ref 20 are summarized in Table 1.

2.2. Methods. *FTIR Spectroscopy*. To verify the concentration of PhenethylPOSS in the prepared nanocomposites, FTIR spectroscopy was employed. The infrared spectra of the samples were recorded by a Thermo-Nicolet (Nexus 670) FTIR spectrometer at room temperature. The nanocomposites were measured in transmission, while the IR spectrum of pure PhenethylPOSS was measured by the ATR-IR technique because PhenethylPOSS is a viscous liquid at room temperature. The measurements were carried out in the wavenumber range from 400 to 4000 cm^{-1}, accumulating 64 scans having a resolution of 2 cm^{-1}.

Gas Permeability. To measure the permeability of CO_2 the time-lag method[34] was applied in the upstream pressure (p_1) range from 1.0 to 20 bar using a temperature controlled setup. To achieve the correct boundary conditions (initial zero gas concentration) and to ensure reproducibility, the samples were degassed prior to the measurements using a turbomolecular

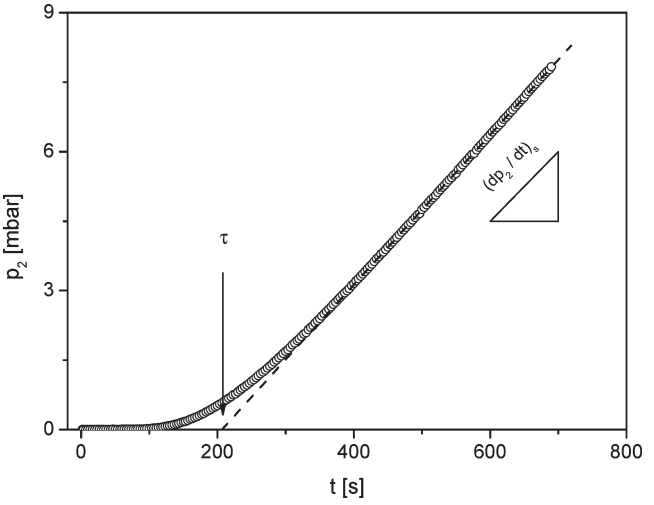

Figure 2. Example for a time-lag measurement: Downstream pressure p_2 vs time for the permeation of CO_2 through pure PBAC at $T = 308$ K for $p_1 = 10$ bar.

vacuum pump system ($< 10^{-5}$ mbar). Prior to the first measurement after film preparation degassing was performed for at least 72 h in order to remove any sorbates as well as remaining solvent traces. In the permeation cell sample films of 38 mm diameter were used and sealed with a Viton O-ring determinig the effective area of $A = 7.07$ cm^2. The pressure increase in the closed downstream volume (p_2) attached to the permeation cell was measured by a temperature-controlled (373 K) MKS Baratron gauge (128 A, 10 mbar range) and recorded together with upstream pressure and temperature.

Figure 2 gives an example for a time-lag measurement for the permeation of CO_2 through pure PBAC. The permeability P was calculated from the slope of the linear pressure increase in the steady state region according to[34,35]

$$P = \frac{VlT_0}{ATp_1p_0}\left(\frac{dp_2}{dt}\right)_s \quad (1)$$

with V = downstream volume, T = temperature, l = sample thickness, $T_0 = 273.15$ K, A = sample area, p_1 = upstream pressure, $p_0 = 1.013$ bar, $(dp_2/dt)_s$ = steady state downstream pressure increase. The permeability coefficients are given in barrer:

$$1 \text{ barrer} = 10^{-10}\left[\frac{\text{cm}^3\ (\text{STP})\ \text{cm}}{\text{cm}^2\ \text{cmHg s}}\right]$$

Permeation experiments were performed in the pressure range from 1.0 to 20 bar at temperatures of 308, 318, 328, and 338 K.

The linear extrapolation of $p_2(t)$ in the steady state region to $p_2 = 0$ gives further the time-lag τ (see Figure 2) which characterizes the initial transient part of the permeation. This time-lag allows the determination of a diffusion coefficient which is considered as effective value D_{eff} due to the pressure or concentration dependence of gas diffusivities in glassy polymers and the resulting variation along the film cross-section[35]

$$D_{\text{eff}} = \frac{l^2}{6\tau} \quad (2)$$

Gas Sorption. Gas sorption was measured gravimetrically using an electronic high pressure microbalance (Sartorius 4406) placed in a temperature controlled air-bath. Like the device for measuring the permeability this apparatus is also equipped with a turbomolecular vacuum pump for degassing. Sorption isotherms in the pressure range from 1.0 to 50 bar were determined from the sum of mass uptakes (corrected for buoyancy effects) in successive steps of pressure increase in the system. The recorded kinetics of the individual mass uptake curves allows furthermore the calculation of diffusion coefficients.[36] Assuming Fickian diffusion the time dependence sample mass m_t after a single pressure step is given by

$$\frac{m_t}{m_\infty} = 1 - \frac{8}{\pi^2}\sum_{n=0}^{\infty}\frac{1}{(2n+1)^2}\exp\left(-\frac{D(2n+1)^2\pi^2}{l^2}t\right) \quad (3)$$

where m_∞ is the mass of the sample for $t \rightarrow \infty$ after a pressure jump. D is the diffusion coefficient, which can be determined by fitting eq 3 (series approximation) to the time dependent data.

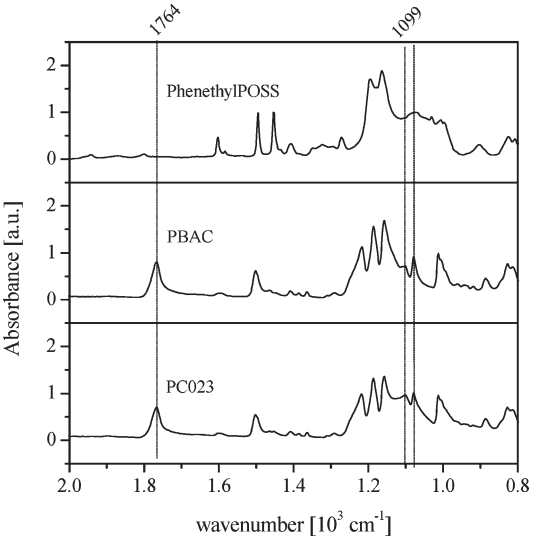

Figure 3. IR spectra of PhenethylPOSS, polycarbonate, and a PBAC-based nanocomposite with 23.1 wt % POSS (PC023).

3. Results and Discussion

FTIR Spectroscopy. Infrared spectroscopy was applied to check whether the content of PhenethylPOSS in the nanocomposite films is the same as in the formulated solution. The IR spectra of the pure poly(bisphenol A carbonate), PhenethylPOSS and a nanocomposite with 23.1 wt % POSS are shown in Figure 3. The absorption band at 1764 cm^{-1} is assigned to the C=O groups in the polycarbonate and is related to the content of the PBAC in the composite. According to the literature,[37−39] the characteristic band of −Si−O−Si− vibrations appears around 1100 cm^{-1} and corresponds to the observed peak at about 1099 cm^{-1} for the bulk PhenethylPOSS (see Figure 3). Blending POSS molecules into the matrix polymer slightly shifts this band to higher wave numbers (1100 cm^{-1}). Its intensity increases with the POSS concentration and therefore this band is used to characterize the content of POSS in the nanocomposite materials.

After subtraction of a baseline, the intensity of the bands at 1100 and 1764 cm^{-1} is estimated by fitting a Gaussian to the data. An example for the fitting procedure is given in Figure 4a. The ratio of the intensities of theses two bands I_{1100}/I_{1764} is plotted versus the molar fraction of PhenethylPOSS (x_{POSS}) in the formulated solution in Figure 4b. This ratio increases linearly with the molar fraction of POSS in the formulation:

$$\left(\frac{I_{1100}}{I_{1764}}\right) = 0.509 \times x_{\text{POSS}} \quad (4)$$

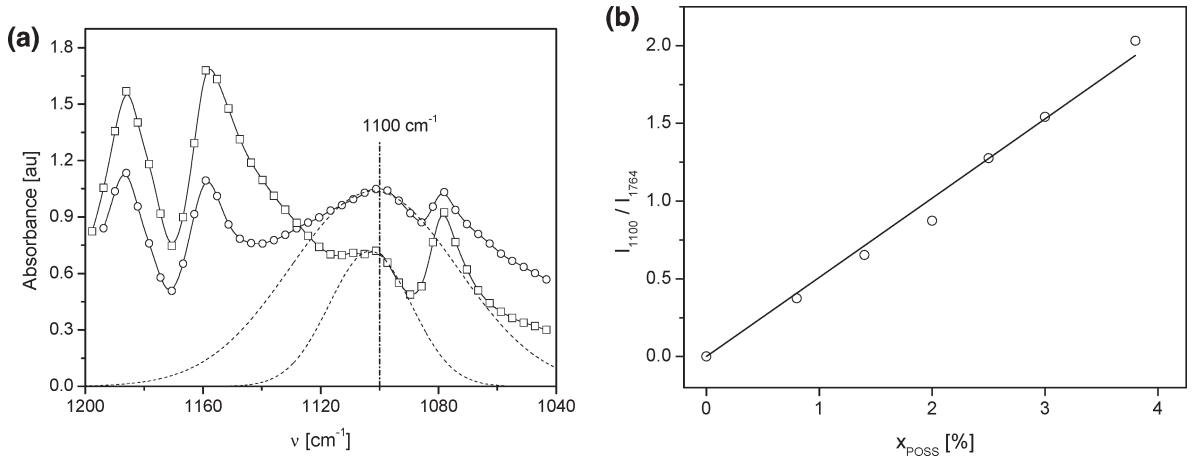

Figure 4. (a) Example for the analysis of the −Si−O−Si− vibration band at 1100 cm^{-1} for pure polycarbonate (squares) and the nanocomposite with 28.6 wt % POSS (circles, PC029). The dashed lines correspond to the fitted Gaussians. (b) Ratio of the FTIR intensities I_{1100}/I_{1764} vs molar fraction of POSS x_{POSS}. The line is a linear regression to the data.

This linear relationship proves that the molar concentration of the POSS in the formed nanocomposite is linearly related to that in the casting solution.

Dielectric Spectroscopy. Dielectric spectroscopy was employed by us to investigate the structure/property relationships of the described nanocomposites recently.[20] To discuss the gas transport properties of CO_2 of these systems in its structure dependence the main results of the dielectric study will be summarized here briefly. For low concentrations of POSS (< 10 wt %) the dielectric spectra of the nanocomposite shows two well-defined relaxation processes a β-relaxation which is due to localized molecular fluctuations at lower temperatures (higher frequencies) and the dynamic glass transition (α-relaxation) due to segmental mobility at higher temperatures (lower frequencies). With increasing concentration of POSS the α-relaxation shifts to lower temperatures in comparison to pure unfilled polycarbonate. This indicates that POSS is dispersed homogenously in the polycarbonate matrix on a molecular level. The main effect of POSS at these low concentrations is the plasticization of the polymeric matrix. Also the β-relaxation shifts with increasing concentration of POSS to lower temperatures. From that one can conclude that the mechanism of plasticization of the polycarbonate matrix by POSS is quite different from that of low molecular weight plasticizers where the opposite effect is observed.

By increasing the concentration of PhenethylPOSS above a critical value c_{POSS}^{crit}, the dielectric spectra shows besides the dielectric behavior discussed for low concentrations two additional relaxation processes (processes II and III; see Figure 10 in ref 20). From this multiple peak structure in the dielectric spectra one has to conclude that a phase separation takes place for higher concentrations of POSS. From a phase diagram where the glass transition temperature is plotted versus the concentration of POSS a miscibility criteria can be deduced by comparing the experimental values with those calculated from the Fox/Flory equation which is expected to be valid for a system which is miscible on a molecular level. For c_{POSS}^{crit} a value of ca. 7−10 wt % is obtained by these considerations. A detailed analysis of the dielectric spectra leads to the following model regarding the structure of the nanocomposites. The first new relaxation mode (process III) is located close to the dynamic glass transition of pure Phenethyl-POSS. Its dielectric strength increases with increasing concentration of POSS. Hence, process III is unambiguously related to bulk-like POSS molecules organized in POSS-rich domains. Therefore, for concentrations higher than c_{POSS}^{crit} the morphology of the nanocomposite consists of a polycarbonate-rich matrix and POSS-rich domains. The dielectric spectra in the temperature range related to relaxation processes of polycarbonate show a double peak structure (process I and process II; see Figure 10 and inset of Figure 8 in ref 20). From the analysis of the concentration dependence of process I, it is concluded that it must be assigned straightforward to the glass transition of the PBAC-rich matrix with 7 wt % POSS dispersed on a molecular level. Process II is located at slightly lower temperatures (or higher frequencies) than Process I. Therefore, it is concluded that this process is related mainly to polycarbonate involving more POSS molecules than process I. The number of possible phases at constant pressure and temperature is only two according to the Gibbs phase rule. Therefore, it is concluded that the POSS-rich domains are surrounded by an interfacial layer consisting mainly of polycarbonate with molecular solved POSS but at a higher concentration than the polycarbonate-rich matrix. Probably this layer has no sharp phase boundaries but corresponds to an interfacial area with a gradient of the POSS concentration. To have a signature as an α-relaxation in the dielectric spectra the interfacial layer must have a certain spatial extent. To allow for the observed glassy dynamics, the characteristic size of this interphase is expected to be in the range between 1 and 3 nm.[40−42] It is worth to note that this model is in agreement with a quite recent structural investigation of melt blended PhenethylPOSS/polycarbonate nanocomposites involving TEM and X-ray studies.[28]

Gas Permeability. The driving force for gas transport is the concentration gradient of the gas molecules across the sample due to a pressure difference between its upstream and downstream side. The transport of small molecules through nonporous amorphous polymers is generally described in terms of a solution-diffusion mechanism consisting of: (1) the sorption of molecules at the upstream side (described by the solubility coefficient S), (2) the diffusive transport across the polymer (diffusion coefficient D) and (3) the desorption at the downstream side. The overall transport, characterized by the permeability coefficient P, is given by

$$P = D \times S \tag{5}$$

Figure 5 gives the permeability P of CO_2 in the investigated nanocomposites versus upstream pressure p_1 and the concentration of PhenethylPOSS at T = 308 K in a 3D-representation. As expected for glassy polymers, P

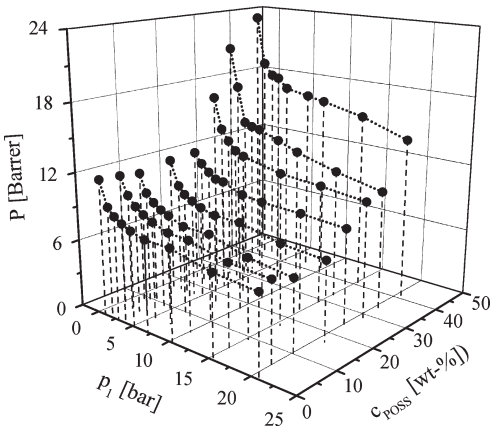

Figure 5. Permeability of CO_2 vs upstream pressure p_1 and concentration of PhenethylPOSS at $T = 308$ K for the investigated nanocomposites.

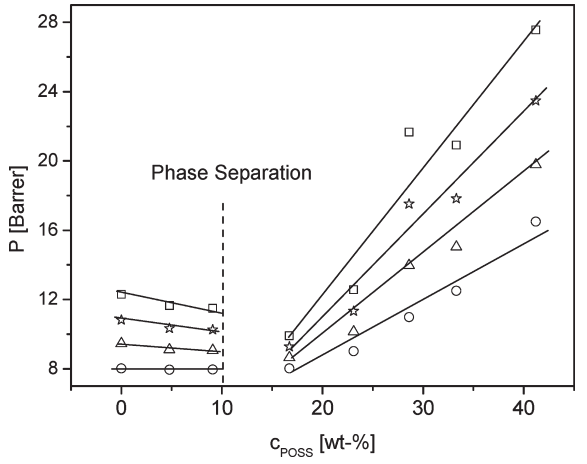

Figure 6. Permeability of CO_2 vs concentration of PhenethylPOSS at 10 bar: circles, $T = 308$ K; triangles, $T = 318$ K; stars, $T = 328$ K; squares, $T = 338$ K. The solid lines are guides for the eyes. The dashed line indicates the concentration where phase separation is expected to set in.

decreaes with increasing upstream pressure. Furthermore, at higher POSS-concentrations the permeability increases moderately with increasing concentration c_{POSS}.

This behavior can be seen more clearly from Figure 6 where P is plotted versus concentration of POSS for an upstream pressure of $p_1 = 10$ bar and different temperatures. For low concentrations of the nanofiller P, seems to be approximately constant (or slightly decreasing) for all temperatures up to a POSS content of ca. 10 wt %. For higher POSS concentrations the permeability increases more or less linearly with the content of the nanofiller.

Gas diffusivity and solubility from permeation experiments. Using the time-lag τ obtained from permeation experiments an effective diffusion coefficient D_{eff} can be calculated (see eq 2) and plotted versus concentration of PhenethylPOSS for several temperatures in Figure 7. The results show a close similarity to the concentration dependence of the permeability P. For low concentrations of POSS, D_{eff} is approximately constant but increases significantly with increasing content of the nanofiller in the range of $c_{POSS} \geq 10$ wt %. An example for such a behavior is also found in ref 27 by molecular dynamics simulations of the structure of POSS/poly(methyl methacrylate) nanocomposites and the diffusion of oxygen therein. Using eq 5, the solubility coefficient S can be calculated from the permeability P and the diffusion

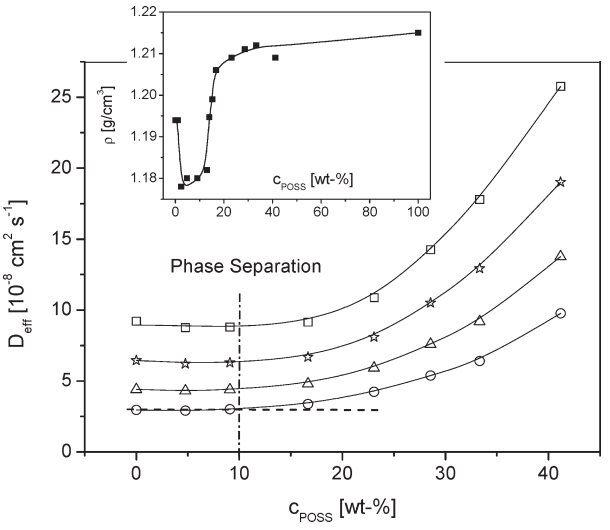

Figure 7. Effective diffusion coefficient D_{eff} vs concentration of PhenethylPOSS obtained from permeation measurements at 10 bar: circles, $T = 308$ K; triangles, $T = 318$ K; stars, $T = 328$ K; squares, $T = 338$ K. The solid lines are guides for the eyes. The dashed line gives the concentration range were D_{eff} is constant. The dashed-dotted line symbolizes the concentration for phase separation. The inset gives the density ρ vs concentration of PhenethylPOSS reported in ref 20. The line is a guide for the eyes.

coefficient D_{eff} obtained from time-lag experiments (see Figure 8a). According to these data, S decreases with increasing concentration of PhenethylPOSS. A similar behavior is observed for the other temperatures measured, which will be discussed in more detail now.

It is obvious to relate the change in the concentration dependence of both, the permeability and the diffusion coefficient, to the nanophase separated structure of the nanocomposites for POSS concentrations higher than c^{crit}_{POSS} discussed above (see the paragraph on dielectric spectroscopy). One has to keep in mind that the determination of permeability and diffusivity from the time-lag data according to eqs 1 and 2 is based on the assumption of a homogeneous sample. Concerning our model for the investigated PC/POSS nanocomposites derived from dynamic and structural features revealed by dielectric relaxation spectroscopy and density measurements[20] this holds only for concentrations of POSS smaller than c^{crit}_{POSS}. For these concentrations a molecular dispersion is found for POSS in the polycarbonate matrix. For higher concentrations than c^{crit}_{POSS}, a nanophase separated structure has to be considered with domains of different solubilities and diffusivities for gas molecules. As already stated a decreasing solubility with increasing POSS concentration is observed (see Figure 8a). A closer inspection of Figure 8a reveals that S may be extrapolated to zero for 100% of POSS content. This indicates that the solubility of CO_2 in PhenethylPOSS is zero or at least essentially smaller than in polycarbonate. Taking this into consideration it can be stated that in the nanophase separated state of the nanocomposites CO_2 is predominately solved in the polycarbonate matrix. In contrast to that the solubility values given in Figure 8 are calculated assuming that carbon dioxide is homogenously solved throughout the whole sample volume V_{Sample}. On the basis of these findings a correction can be suggested and performed which only accounts for the volume fraction which is effectively available for gas sorption and transport which is the volume of the polymeric matrix $V_{Polymer}$. Assuming in a simplified two phase model that the CO_2 solubility is zero in the PhenethylPOSS-rich domains

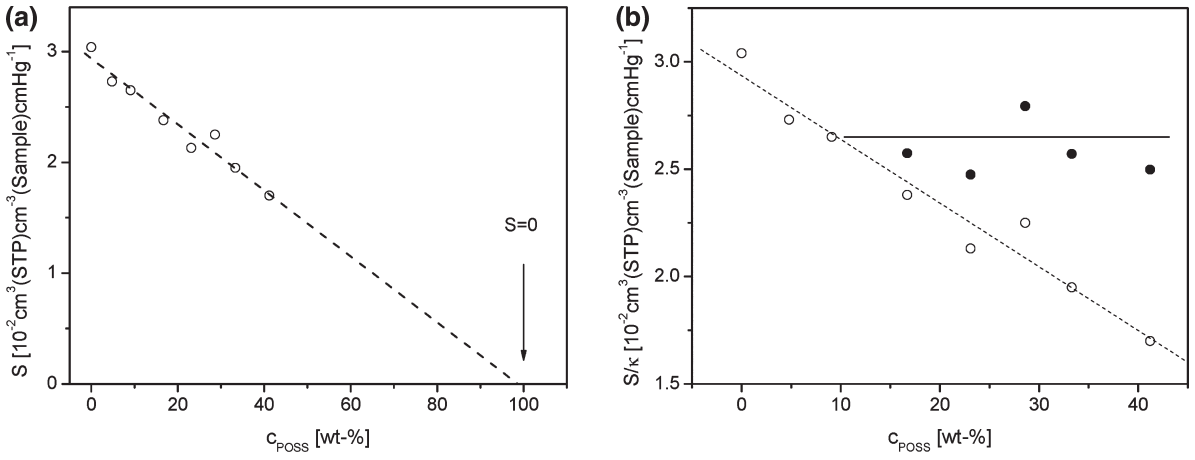

Figure 8. (a) Solubility S vs the concentration of PhenethylPOSS at 10 bar for $T = 308$ K. (b) Comparison between the volume corrected values of the solubility (solid circles) with the uncorrected ones (open circles). The solid line is a guide for the eyes. The dashed line in both cases is a linear regression to the uncorrected data.

with the volume V_{Domain} and furthermore an additive behavior, it holds that

$$V_{\mathrm{Polymer}} = V_{\mathrm{Sample}} - V_{\mathrm{Domain}} \tag{6}$$

Invoking the nanophase separated morphology deduced from dielectric spectroscopy,[20] one can formulate for V_{Domain}

$$V_{\mathrm{Domain}} = \begin{cases} 0 & \text{for } c_{\mathrm{POSS}} \le c_{\mathrm{POSS}}^{\mathrm{crit}} \\ \dfrac{(m_{\mathrm{POSS}} - m_{\mathrm{POSS}}^{\mathrm{crit}})}{\rho_{\mathrm{POSS}}} = \dfrac{(c_{\mathrm{POSS}} - c_{\mathrm{POSS}}^{\mathrm{crit}})}{\rho_{\mathrm{POSS}}} m_{\mathrm{sample}} & \text{for } c_{\mathrm{POSS}} > c_{\mathrm{POSS}}^{\mathrm{crit}} \end{cases} \tag{7}$$

Here m_{POSS} is the mass of POSS belonging to c_{POSS}, ρ_{POSS} is the density of PhenethylPOSS and m_{Sample} the mass of the whole system. Assuming that the density of the POSS-rich domains may be approximated by the density of bulk POSS and considering $m_{\mathrm{Sample}} = \rho(c_{\mathrm{POSS}})V_{\mathrm{Sample}}$ for the volume correction κ of the solubility

$$\kappa = \frac{V_{\mathrm{Polymer}}}{V_{\mathrm{Sample}}} = 1 - \frac{V_{\mathrm{Domain}}}{V_{\mathrm{Sample}}}$$

$$\approx 1 - \frac{\rho(c_{\mathrm{POSS}})}{\rho_{\mathrm{POSS}}}(c_{\mathrm{POSS}} - c_{\mathrm{POSS}}^{\mathrm{crit}}) \quad \text{for } c_{\mathrm{POSS}} > c_{\mathrm{POSS}}^{\mathrm{crit}} \tag{8}$$

is obtained. $\rho(c_{\mathrm{POSS}})$ is the density of the system in dependence on the concentration of PhenethylPOSS (see Tab. 1, inset Figure 7). Applying this approach to the solubility data leads to constant values of the CO_2-solubility obtained from time-lag experiments at 308 K for POSS concentrations higher than $c_{\mathrm{POSSI}}^{\mathrm{crit}}$ (see Figure 8b), which in turn is a confirmation of the nanophase separated morphology discussed above. For $c \le c_{\mathrm{POSS}}^{\mathrm{crit}}$ the solubility decreases with increasing concentration of the nanofiller because at these low concentrations POSS is dispersed in to the polycarbonate matrix on a molecular level. For $c > c_{\mathrm{POSS}}^{\mathrm{crit}}$, nanophase separation occurs, the concentration of POSS in the polycarbonate matrix remains constant at $c_{\mathrm{POSSI}}^{\mathrm{crit}}$ and therefore a constant solubility for CO_2 is found. For the other temperatures considered in this study a similar behavior is observed.

In contrast to the solubility the concentration dependence of the diffusivity cannot be discussed in the framework of such a simple model (cf. Figure 7). The diffusivity depends on both the effective length of the diffusion pathways and the molecular mobility of the polymer matrix. Both properties depend in a delicate manner on the actual morphology of the nanocomposites. For concentrations below $c_{\mathrm{POSS}}^{\mathrm{crit}}$, the diffusion coefficient is more or less independent from the concentration but increases strongly for $c_{\mathrm{POSS}} > c_{\mathrm{POSS}}^{\mathrm{crit}}$. Therefore, in general the increase of D_{eff} above $c_{\mathrm{POSS}}^{\mathrm{crit}}$ should also be related to the phase separated structure. From dielectric spectroscopy, it is deduced that in the phase separated state the nanocomposites consist of a polycarbonate-rich matrix (1) which contains a certain level of molecularly solved POSS and POSS-rich domains (2) the latter being surrounded by an interfacial layer (3) with a higher concentration of POSS and a higher molecular mobility than the polycarbonate-rich matrix (see paragraph on dielectric spectroscopy). Therefore, the simplified two phase model used for correcting the CO_2-solubility data is not appropriate to describe the diffusion behavior of gas molecules which is strongly related to the dynamics of the local surrounding within the polymeric matrix.

So on one hand, the length of the effective diffusion pathways is changed due to the nanophase separated structure and the presence of POSS-rich domains (2) throughout the matrix. As these domains are considered impermeable (CO_2 solubility effectively zero), longer pathways are expected due to increased tortuosity. Moreover it was stated above that in the polycarbonate-rich matrix (1) the solubility of CO_2 is approximately constant (see inset Figure 8). Therefore, the observed increase in the diffusivity above the critical POSS concentration may not be related to a CO_2 induced plasticization of the polycarbonate-rich matrix as it remains essentially unchanged compared to its state at the critical POSS concentration. But as discussed above the POSS-rich domains are surrounded by an interfacial layer (3) having an essentially higher molecular mobility than the polycarbonate-rich matrix (1). As this interfacial layer consists mainly of polycarbonate, CO_2 can be dissolved in these interphase regions and because of the higher molecular mobility the diffusion is enhanced.

With increasing concentration of POSS, the size and/or the number of the POSS-rich domains increases and therefore also the amount of the discussed interphase. For higher concentrations of POSS this interfacial regions may also form larger areas with higher mobility or even percolate to high mobility channels for faster diffusion. Therefore, the increase of D_{eff} with the concentration of POSS in

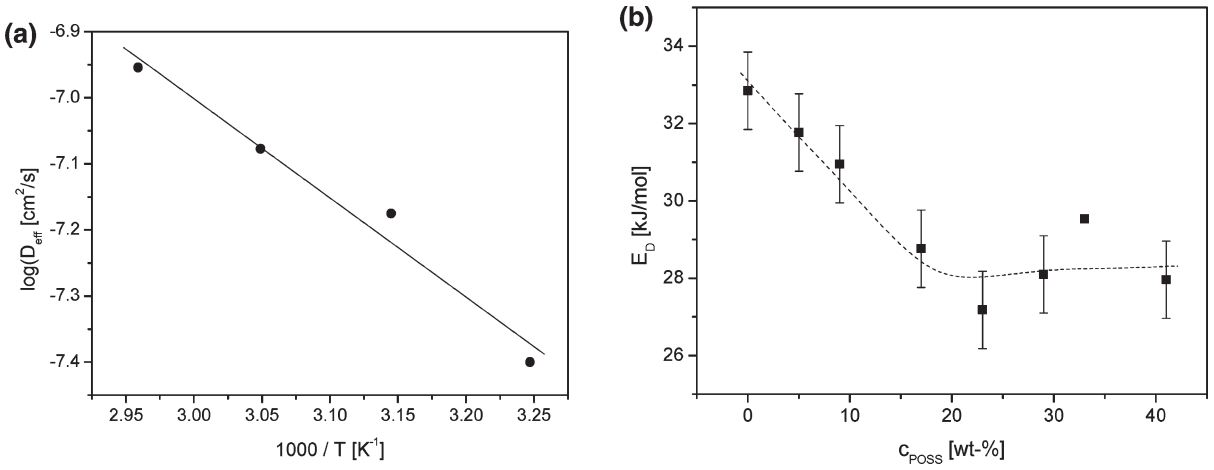

Figure 9. (a) Effective diffusion coefficient D_{eff} versus inverse temperature for the nanocomposite with 33 wt % PhenethylPOSS. The line is a fit of the Arrhenius equation to the data. (b) Activation energy E_{D} for diffusion versus the concentration of POSS. The line is a guide to the eyes.

the nanophase separated state may be assigned to the increasing amount of interfacial area with a higher molecular mobility than the polycarbonate-rich matrix. It should be noted that this line of argumentation is in agreement with molecular dynamic simulations which predict a higher molecular mobility close to the POSS particles in related systems[26] and also channel-like structures with higher gas diffusion.[27]

Activation Energy of Diffusion. Correlation with Dielectric Spectroscopy. The effective diffusion coefficient D_{eff} was determined from time-lag measurements for each POSS concentration at four different temperatures. An example for that is given in Figure 9a for $p = 10$ bar. The temperature dependence of the effective diffusion coefficients D_{eff} can be described by an Arrhenius (Figure 9a) relation allowing the calculation of the corresponding activation energy of the diffusion E_{D}.

$$D_{eff} = D_{eff,0} \exp\left(-\frac{E_{\text{D}}}{RT}\right) \tag{9}$$

where T is the temperature, R is the molar gas constant, and $D_{\text{eff},0}$ is the diffusion coefficient for $T \rightarrow \infty$ (pre-exponential factor).

In Figure 9b, the resulting activation energy E_D for diffusion is plotted versus the concentration of PhenethylPOSS. For $c_{\text{POSS}} < c^{\text{crit}}_{\text{POSS}}$ E_{D} decreases with increasing POSS concentration but becomes approximately constant for $c_{\text{POSS}} > c^{\text{crit}}_{\text{POSS}}$.

As already pointed out the dielectric relaxation behavior of the PC/POSS nanocomposites under investigation was discussed in detail recently.[20] Pure polycarbonate shows besides the dynamic glass transition (α-relaxation) a β-process at lower temperatures/higher frequencies which corresponds to localized molecular fluctuations. With increasing concentration of PhenethylPOSS this β-peak shifts to lower temperatures/higher frequencies in comparison to the bulk. The quantitative analysis of this relaxation process shows that the temperature dependence of the relaxation rate follows an Arrhenius law as expected. The concentration dependence of the estimated activation energies E_{A} shows a close similarity to that of E_{D} (see inset of Figure 10). First, one has to note that the activation energy for the CO_2 diffusion is a bit lower than that for the dielectric β-relaxation. In Figure 10 the activation energy E_{D} for the CO_2 diffusion is plotted versus E_{A} of the β-process. Both sets of data which are measured completely independent from each other correlate well, and the relationship between both can be described by a straight line. From this correlation one has to conclude that both the gas transport and the dielectric β-relaxation in these systems are controlled by the same molecular process. Because the β-process is assigned to localized molecular fluctuations it is reasoned that also the gas transport is controlled by the same molecular motions. In order to further prove this conclusion more experiments need to be carried out for different gases and = more importantly = on a series of different materials.

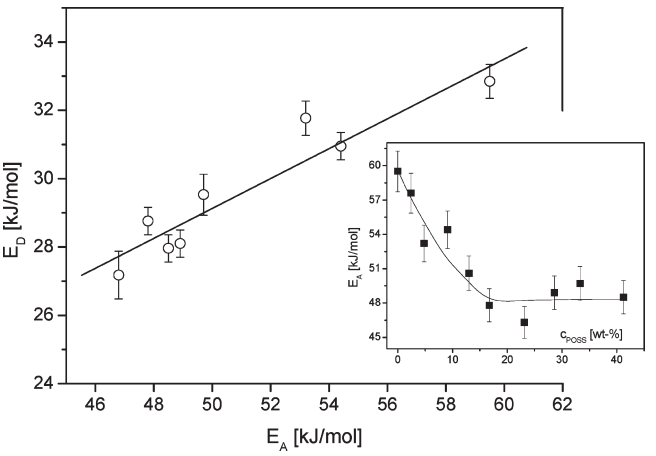

Figure 10. Activation energy E_{D} for diffusion versus the activation energy E_{A} for the β-relaxation estimated by dielectric spectroscopy. The line is a linear regression to the data. The regression coefficient is $r = 0.94$. The inset gives the activation energy E_{A} for the β-relaxation versus the concentration of PhenethylPOSS. The data were taken from ref 20. The line is a guide for the eyes.

Gas Sorption. For glassy polymers the gas transport is often discussed in the framework of the *dual mode sorption* model (DMSM)[34,35] describing the sorbed penetrant concentration C as the sum of a Henry-type solubility (C_{D}) and a Langmuir-type sorption (C_{H}), resulting in sorption isotherms concave to the pressure axis (characteristic for glassy polymers) and a decrease of solubility S and permeability P with increasing pressure/concentration. One gets

$$C = C_{\text{D}} + C_{\text{H}} = k_{\text{D}} p_1 + \frac{C_{\text{H}}' \cdot b p_1}{1 + b p_1} \tag{10}$$

where k_{D} is the Henry coefficient, C_{H}' the Langmuir capacity, and b the Langmuir hole affinity constant. The physical

basis of the dual-mode-sorption model is under controversial debate. Therefore, eq 10 is used here only as a tool to represent the data of the concave shaped sorption isotherms. Figure 11 gives the concentration of CO_2 versus pressure p_1 (sorption isotherms) for three different concentrations of POSS at $T = 308$ K. The data for pure polycarbonate can be well described by the DMSM. Also the sorption isotherms for a nanocomposite with ca. 10 wt % POSS shows the concave shape expected for a glassy polymer. One has to bear in mind that 10 wt % PhenethylPOSS is close to c_{POSS}^{crit}. For higher concentrations of POSS, the data follow the dual-mode-sorption model only in the low pressure region (up to 15 bar). For higher pressures, an upturn of the sorption isotherms in comparison to the dual mode curve is observed (see Figure 11), which becomes more pronounced with further increasing POSS concentration. Such an upturn is usually characteristic for a CO_2-induced plasticization. But because the concentration of CO_2 in the polycarbonate-rich matrix is more or less independent from the POSS concentration above c_{POSS}^{crit} and the fact that the deviation from the DMSM model is only observed for the nanophase separated state ($c_{POSS} > c_{POSS}^{crit}$), it must be concluded here that this deviation in the observed CO_2 sorption behavior cannot be ascribed unambiguously to a plasticization of the continuous polymer-rich matrix due to a significantly higher overall CO_2-concentration. Instead this behavior may be explained taking into account that above the critical POSS concentration c_{POSS}^{crit} the interfacial region between the two phases of the phase separated morphology is present and may give rise to the observed sorption deviation. Because of the higher molecular mobility observed for this interphase based on dielectric spectroscopy data it is reasonable to suggest for these regions also a higher tendency to be influenced by locally present CO_2, i.e., a stronger susceptibility to plasticization at higher pressures/concentrations.

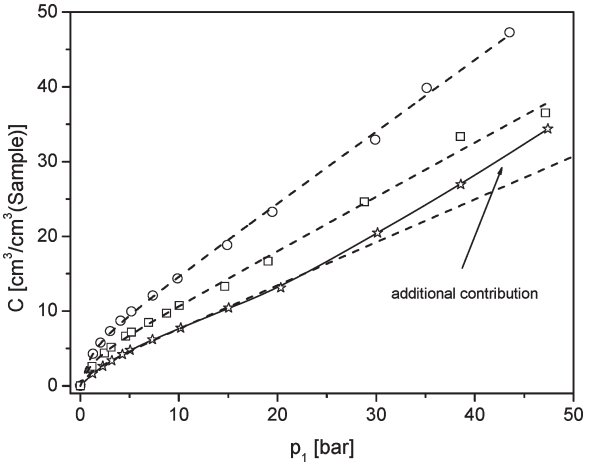

Figure 11. Concentration C of CO_2 versus up stream pressure p_1: circles, pure polycarbonate; squares, 9.1 wt % PhenethylPOSS (PC010); stars, 41.2 wt % PhenethylPOSS (PC041). The dashed lines are fits of the Dual-Mode-Sorption-model to the data. The solid line is a guide for the eyes.

With respect to the solubility data obtained from time-lag data discussed in an earlier section, it should be also noted that the deviations from the dual-mode behavior occur at CO_2 pressures distinctly higher (about 30 bar) than that covered by the permeation experiments (up to 20 bar).

Comparison of Permeation and Sorption Experiments. As discussed above a diffusion coefficient can be estimated either from time-lag data (D_{eff}) obtained from permeation measurements or by evaluating the Fickian kinetics from sorption data applying eq 3. Figure 12a compares these two diffusion coefficients in dependence of the concentration of POSS in the nanocomposite materials. Both sets of data measured completely independent from each other show a good agreement with regard to both their absolute values and their concentration dependence. It has to be noted that the underlying experimental methods apply different boundary conditions, i.e., a finally uniform gas concentration throughout the sample in the case of sorption and in the case of time-lag permeation measurements a concentration gradient along the film's cross-section between upstream gas pressure and downstream vacuum. Moreover one has to note that the effective diffusion coefficient derived from the time-lag of the permeation experiment corresponds to a transient nonequilibrium state and not the steady state (see Figure 2).

For the sorption experiments also the solubility S can be derived by dividing the concentration of the sorbed gas by the corresponding pressure (secant slope of the respective data point of the sorption isotherm). Figure 12b compares the solubility estimated from permeation and sorption measurements at 10 bar versus the concentration of POSS. First one has to note that the absolute values of both data sets measured completely independent are different. The reasons for that result are again the different boundary conditions and the different states of the sample. As discussed for

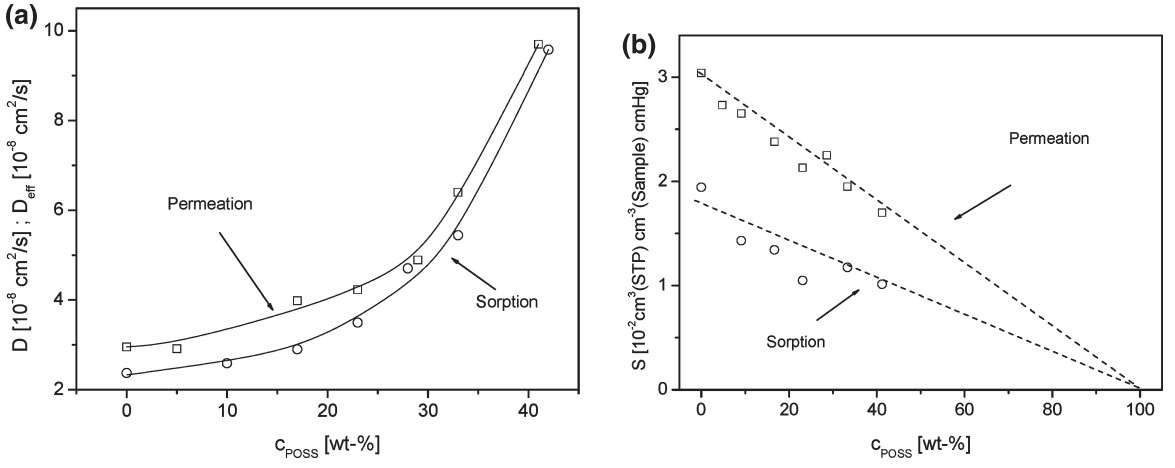

Figure 12. (a) Comparison of the diffusion coefficient estimated from the time-lag τ (squares) with that measured by sorption experiments (circles) versus the POSS concentration at a pressure of 10 bar. (b) Comparison of the solubility estimated from permeation measurements (squares) with that measured by sorption experiments (circles) versus the POSS concentration at a pressure of 10 bar. The lines are guides for the eyes.

the diffusion coefficients in the permeation experiment a concentration gradient across the sample's cross-section is reached in the steady state with a constant permeation rate (from which the permeability coefficient is determined). The effective diffusion coefficient is estimated from the transient nonsteady state period which is necessary to establish the final concentration gradient starting from a completely degassed film. For the sorption experiments the final gas concentration is uniform and the sample is in a (pseudo)-equilibrium with the surrounding gas phase. For these reasons it is not to be expected that both data sets agree in their absolute values. But second—and more important—both sets of data exhibit the same dependence on the concentration of POSS and end up at zero for an extrapolation to 100% POSS. This shows that permeation and sorption measurements are consistent which each other.

Conclusion

In this paper, we presented results from gas transport investigations, i.e., permeation and sorption experiments with CO_2 for a polymer based nanocomposite systems consisting of polycarbonate and Phenethyl-POSS as nanofiller. These experiments were performed complementary to a comprehensive dielectric spectroscopy study published earlier.[20] With this approach we were able to support most of the conclusions drawn about structure and dynamics in the PC/POSS nanocomposites under investigation based on their dielectric relaxation behavior by evaluation of sorption and diffusion coefficients obtained for different POSS-concentrations. First, the occurrence of a phase separated structure above a critical POSS-concentration of about 7 wt % was confirmed by permeability and diffusivity results obtained from permeation experiments as well as by deviations in the sorption behavior at higher CO_2 pressures. Second, completely new insights are provided concerning the importance of the interfacial area between a nanoparticle or its aggregated domains and the polymeric matrix for the gas transport properties of CO_2. These new experimental results and considerations are in agreement with recent molecular dynamic simulations concerning the structure and the gas transport properties of a related nanocomposites with POSS as nanofiller.[27] Furthermore, a consistent discussion of the gas solubility determined from permeation measurements was possible assuming impermeable POSS-rich domains due their CO_2 solubility being practically zero.

Finally a correlation between the activation energies of the ss-relaxation process in the polymeric matrix of the nanocomposites and the CO_2 diffusivity was estimated, suggesting that both are correspond to the same local molecular motions.

Acknowledgment. The authors gratefully acknowledge the assistance of Dr. O. Hölck and D. Neubert for their experimental help. The financial support from the Ph.D. program of BAM to N.H. is highly appreciated.

References and Notes

(1) LeBaron, P. C.; Wang, Z.; Pinnavaia, T. J. *Appl. Clay Sci.* **1999**, *15*, 11.
(2) Alexandre, M.; Dubois, P. *Mater. Sci. Eng.* **2000**, *28*, 1.
(3) Krishnamoorti, R.; Vaia, R. A. Polymer Nanocomposites. In *ACS Symposuim Series*; Amercian Chemical Society: Washington, DC, 2002; Vol. *804*.
(4) Sinha Ray, S.; Okamoto, M. *Prog. Polym. Sci.* **2003**, *28*, 1539.
(5) Leuteritz, A.; Kretzschmar, B.; Pospiech, D.; Costa, R. F.; Wagenknecht, U.; Heinrich, G. Industry-relevant preparation, characterization and applications of polymer nanocomposites. In: *Polymeric nanostructures and their applications*; Nalwa, H. S., Ed.; American Scientific Publishers: Los Angeles, CA, 2007.
(6) Böhning, M.; Goering, H.; Fritz, A.; Brzezinka, K. W.; Turky, G.; Schönhals, A.; Schartel, B. *Macromolecules* **2005**, *38*, 2764.
(7) POSS and PhenethylPOSS are trade marks for Polyhedral Oligomeric Silsesquioxane and phenethyl-silsesquioxane (MS0870) of Hybrid Plastics Inc. (Hattiesburg, MS, USA), respectively. See also www.hybridplastics.com
(8) Lichtenhan, J. D.; Schwab, J. J.; Reinerth, W. A. *Chem. Innov.* **2001**, *31*, 3.
(9) Joshi, M.; Butola, B. S. *J. Macromol. Sci. B Polym. Rev.* **2004**, *C44*, 389.
(10) Zhao, Y. Q.; Schiraldi, D. A. *Polymer* **2005**, *46*, 11640.
(11) Haddad, T. S.; Lichtenhan, J. D. *J. Inorg. Organomet. Polym.* **1995**, *5*, 237.
(12) Fina, A.; Tabuani, D.; Frache, A.; Camino, G. *Polymer* **2005**, *46*, 7855.
(13) Fina, A.; Abbenhuis, H. C. L.; Tabuani, D.; Frache, A.; Camino, G. *Polym. Degrad. Stab.* **2006**, *91*, 1064.
(14) Fu, B. X.; Yang, L.; Somani, R. H.; Zong, S. X.; Hsiao, B. S.; Phillips, S.; Blanski, R.; Ruth, P. *J. Polym. Sci., B: Polym. Phys.* **2001**, *39*, 2727.
(15) Kopesky, E. T.; Boyes, S. G.; Treat, N.; Cohen, R. E.; McKinley, G. H. *Rheol. Acta* **2006**, *45*, 971.
(16) Kopesky, E. T.; McKinley, G. H.; Cohen, R. E. *Polymer* **2006**, *47*, 299.
(17) Soong, S. Y.; Cohen, R. E.; Boyce, M. C. *Polymer* **2007**, *48*, 1410.
(18) Bian, Yu.; Pejanović, S.; Kenny, J.; Mijovic, J. *Macromolecules* **2007**, *40*, 6239.
(19) Hao, N.; Böhning, M.; Schönhals, A. *Macromolecules* **2007**, *40*, 9672.
(20) Hao, N.; Böhning, M.; Goering, H.; Schönhals, A. *Macromolecules* **2007**, *40*, 2955.
(21) Phillips, S. H.; Haddad, T. S.; Tomczak, S. J. *Curr. Opin. Solid State Mol.* **2004**, *8*, 21.
(22) Blanski, R. L.; Phillips, S. H.; Chaffee, K.; Lichtenhan, J. D.; Lee, A.; Geng, H. P. *Mat. Res. Symp. Proc.* **2000**, *628*, cc6.27.
(23) Kopesky, E. T.; Haddad, T. S.; Cohen, R. E.; McKinley, G. H. *Macromolecules* **2004**, *37*, 8992.
(24) Kopesky, E. T.; Haddad, T. S.; McKinley, G. H.; Cohen, R. E. *Polymer* **2005**, *46*, 4743.
(25) Pracella, M.; Chionna, D.; Fina, A.; Tabuani, D.; Frache, A.; Camino, G. *Macromol. Symp.* **2006**, *234*, 59.
(26) Bizet, S.; Galy, J.; Gèrard, J. F. *Polymer* **2006**, *47*, 8219.
(27) Zhang, Q. G.; Liu, Q. L.; Wu, J. Y.; Chen, Y.; Zhu, A. M. *J. Membr. Sci.* **2009**, *342*, 1005.
(28) Sanchez-Soto, M.; Schiraldi, D. A.; Illescas, S. *Eur. Polym. J.* **2009**, *45*, 341.
(29) Merkel, T. C.; He, Z.; Pinnau, I.; Freeman, B. D.; Meakin, P.; Hill, A. J. *Macromolecules* **2003**, *36*, 6844.
(30) Merkel, T. C.; Freeman, B. D.; Spontak, R. J.; He, Z.; Pinnau, I.; Meakin, P.; Hill, A. J. *Science* **2002**, *296*, 519.
(31) Choudalakis, G.; Gotsis, A. D. *Eur. Polym. J.* **2009**, *45*, 967.
(32) Rikowski, E.; Marsmann, H. C. *Polyhedron* **1997**, *19*, 3357.
(33) Bassindale, A. R.; Chen, H. P.; Liu, Z. H.; MacKinnon, L. A.; Parker, D. J.; Taylor, P. G.; Yang, Y. X.; Light, M. E.; Horton, P. N.; Hursthouse, M. B. *J. Organomet. Chem.* **2004**, *689*, 3287.
(34) Petropoulos, J. H. Mechanisms and Theories for Sorption and Diffusion of Gases in Polymers. In: *Polymeric Gas Separation Membranes*; Paul, D. R., Yampol'skii, Y. P., Eds.; CRC Press: Boca Raton, FL, 1994.
(35) Paul, D. R. *Ber. Bunsen-Ges. Phys. Chem.* **1979**, *83*, 294.
(36) Crank, J. *The Mathematics of Diffusion*; Oxford University Press: Oxford, U.K., 1975; Chapter.10.
(37) Lee, L. H.; Chen, W. C. *Polymer* **2005**, *46*, 2163.
(38) Zhang, Y.; Lee, S.; Yoonessi, M.; Liang, K.; Pittman, C. U. *Polymer* **2006**, *47*, 2984.
(39) Ni, Y.; Zheng, S. *Chem. Mater.* **2004**, *16*, 5141.
(40) Fragiadakis, D.; Pissis, P.; Bokobza, L. *Polymer* **2005**, *46*, 6001.
(41) Donth, E. *Relaxation and Thermodynamics in Polymers-Glass Transition*; Akademie-Verlag: Berlin, 1992.
(42) Donth, E.; Huth, H.; Beiner, M. *J. Phys.: Condens. Matter.* **2001**, *13*, L451.